ELSEVIER

Nuclear Physics A 622 (1997) 391–403

NUCLEAR PHYSICS A

Backward yields of pions, protons, and deuterons in relativistic ^{28}Si+Pb collisions at 14.6 A GeV/c

J. Barrette[c], R. Bellwied[h], S. Bennett[h], P. Braun-Munzinger[f], W.E. Cleland[e], T.M. Cormier[h], G. David[a], J. Dee[f], G.E. Diebold[i], O. Dietzsch[g], J.V. Germani[i], S. Gilbert[c], S.V. Greene[i], J.R. Hall[h], T.K. Hemmick[f], N. Herrmann[b], B. Hong[f], K. Jayananda[e], D. Kraus[e], B. Shiva Kumar[i], R. Lacasse[c], Q. Li[h], D. Lissauer[a], W.J. Llope[f], T.W. Ludlam[a], A. Lukaszew[h], R. Majka[i], S.K. Mark[c], R. Matheus[h], S. McCorkle[a], J.T. Mitchell[i], M. Muthuswamy[f], E. O'Brien[a], S. Panitkin[f], C. Pruneau[h], M.N. Rao[f], M. Rosati[c], F. Rotondo[i], N.C. da Silva[g], U. Sonnadara[e], J. Stachel[f], H. Takai[a], E.M. Takagui[g], T.G. Throwe[a], S. Voloshin[e], G. Wang[c], D. Wolfe[d], C.L. Woody[a], N. Xu[f], Y. Zhang[f], Z. Zhang[e], C. Zou[f]

E814 Collaboration

[a] *Brookhaven National Laboratory, Upton, NY 11973, USA*
[b] *Gesellschaft für Schwerionenforschung, Darmstadt, Germany*
[c] *McGill University, Montreal, Canada*
[d] *University of New Mexico, Albuquerque, NM 87131, USA*
[e] *University of Pittsburgh, Pittsburgh, PA 15260, USA*
[f] *SUNY, Stony Brook, NY 11794, USA*
[g] *University of São Paulo, São Paulo, Brazil*
[h] *Wayne State University, Detroit, MI 48202, USA*
[i] *Yale University, New Haven, CT, USA*

Received 23 April 1997; revised 29 May 1997

Abstract

The production of pions, protons and deuterons is studied at a laboratory angle of 144° in ^{28}Si+Pb collisions at 14.6 GeV/c per nucleon. The centrality dependence of the pion yields is studied over the full impact parameter range using a zero degree calorimeter. The results are compared with the hadronic cascade model RQMD. These calculations are generally in agreement with the experimental results. According to these calculations, the pion yield in our acceptance is completely dominated by Δ-decay at freeze-out. Our measurements thus support the importance of baryon resonance production as one of the central features of relativistic heavy ion collisions

PII S0375-9474(96)00326-6

at AGS energies. Although the strength of the pion spectrum is adequately described for kinetic energies above 50 MeV, an additional very soft component is observed in the pion spectra which is not predicted by RQMD. This very soft component accounts for a significant fraction of the total pion yield in this rapidity range but remains unexplained. © 1997 Elsevier Science B.V.

PACS: 25.75.+r
Keywords: Relativistic heavy-ion collision; Backward hemisphere; AGS Si+Pb

1. Introduction

Hadronic cascade calculations as in the RQMD [1] and ARC [2] models have been remarkably successful in explaining a large variety of single-particle observables and two-particle correlations in relativistic heavy ion reaction studies at the AGS [3]. Both the ^{28}Si+Pb and ^{197}Au+^{197}Au systems have been extensively studied. While the success of conventional hadronic physics as contained in these cascade calculations is mainly a consequence of the approach to thermal equilibrium and the expected dominance of conventional hadronic physics during the freeze-out phase of the collision, it does suggest that these models may provide at least a semi-microscopic picture of the later stages of the time evolution of the colliding system. Within this picture, complete, or nearly complete, stopping at AGS energies leads to very high baryon densities, up to 10 times nuclear matter density for the heaviest system, which exist for significant periods of time the hadronic cascade prediction [2,6] of copious production of baryonic resonances, particularly the $\Delta(1232)$, in the collision fireball. The effect of resonance formation on the spectral shape of pion and proton spectra was already pointed out by Brockmann et al. [7] for heavy ion data measured at BEVALAC energies. At AGS energies the Δ density alone is predicted by RQMD to exceed normal nuclear matter density for some time during the collision for the heaviest systems. The consequences of such "resonance matter" for pion production in AGS collisions was first discussed by Brown, Stachel and Welke [8] where it was shown that those pions whose last interaction in the collision zone involve Δ decay (π_Δ) appear "colder" on the average than the balance of the so-called direct pions ($\pi_{\rm dir}$) whose last interaction in the collision involved a non-resonant, non-annihilating scattering from the thermal bath of hadronic matter. The net result of this colder source of Δ decay pions is an enhancement in the pion spectrum which, as shown Ref. [8], accounts for the observed rise in the pion yield at low p_t thus allowing a more nearly consistent determination of an intrinsic temperature for the system.

Experimentally, the direct observation of a distinct low p_t enhancement for negatives (mostly pions) at the AGS was first reported by the E810 Collaboration [9]. Subsequently, the low p_t region has now been studied in considerable detail by the E814 Collaboration [10] for identified pions. In this work, spectra of π^+ and π^-, mostly at forward rapidities ($y > 2.8$), have been measured down to and including $p_t = 0$. The pronounced deviation from a Boltzmann-like spectrum which is observed at low p_t in these measurements is quantitatively accounted for by both ARC and RQMD where it

is shown that pions from baryon-resonance decay, especially the Δ, produce the low p_t anomaly.

In this description of the low p_t enhancement, the yield of Δ's at freeze-out is directly linked to reproducing the full shape of the pion spectra. The E814 Collaboration has also recently measured the Δ^{++} yield directly from the π^+p invariant mass spectrum in their acceptance. The results [10] are in good agreement with RQMD predictions thus lending additional support to the "resonance matter" interpretation of the low p_t pion spectra, at least at these forward rapidities.

Recently, Sorge [6] has noted that Δ decay produces a low p_t enhancement of the pion yield with a characteristic rapidity dependence. Specifically, since the source of Δ decay pions has its greatest density at some rapidity y_0, close to the rapidity at which the baryon density dN/dy peaks in general, the pion spectrum from these Δ decays will show the strongest enhancement at low p_t for y significantly forward or backward of y_0, due to kinematics.

The existing measurements [9,10] of pions at low p_t at the AGS are confined mainly to forward rapidities ($2.2 < y < 2.6$ for E810 and $2.8 < y < 3.6$ for E814) where considerable enhancement above thermal behavior is predicted [6]. As noted above, RQMD and ARC both give an excellent account of the experimentally observed enhancement at these forward rapidities [10]. Clearly it is desirable to also corroborate the very pronounced enhancement predicted for backward pions. The present work, which reports the first measurement of pions at negative rapidity, addresses this part of phase space.

2. Experimental method

We have studied pion, proton and deuteron production in ^{28}Si+Pb collisions at the AGS at 14.6 A GeV/c at a fixed laboratory angle of $\theta = 144°$, corresponding to a fixed pseudo-rapidity of $\eta = -1.1$, using a Si/scintillator telescope added to the E814 apparatus for the 1992 run at the AGS. The full E814 apparatus is described in detail elsewhere [11].

The scintillator detector itself consisted of six ΔE–E scintillator pairs of thickness 5 and 170 mm, respectively. The detector pairs were stacked longitudinally such that a penetrating particle will generate a sequence of dE/dx signals along its track length in alternating thin and thick scintillators. Each particle is identifiable in the scintillator block in which it stops and the preceding ΔE detector. The spectral distribution of incident particles is such that the energy loss in these blocks is confined to the $1/\beta^2$ region where all particles are far from minimum ionizing. In the present experiment this allows clear separation of electrons and pions at all energies of interest. A sample of the linearized ΔE–E spectrum for particles that stop in the first 170 mm scintillator is shown in Fig. 1. The particle identification is based on a simulation of the detector response. For comparison, the pion spectra are shown for two different kinetic energy ranges to illustrate that good pion identification is achieved down to energies of 20 MeV without interference from electrons or other backgrounds. The solid points in Fig. 1

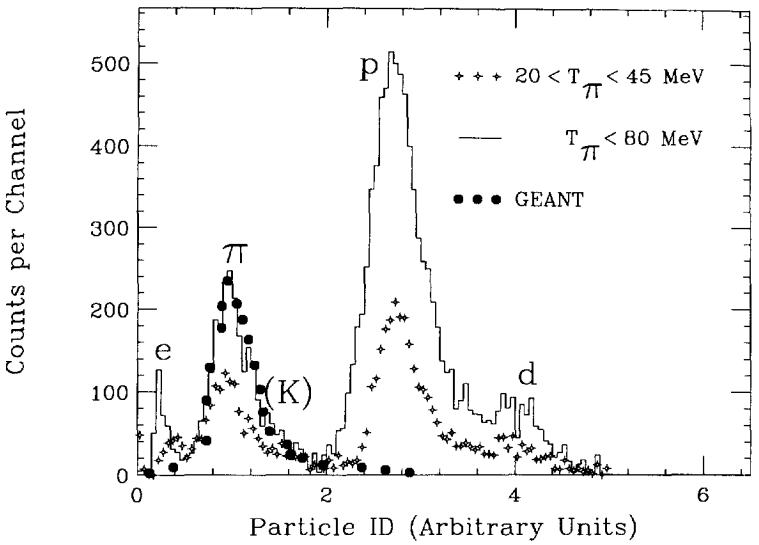

Fig. 1. A sample particle identification spectrum for particles that stop in the first 170 mm scintillator block of the detector. Two kinetic energy cuts are shown. The solid points show the GEANT calculated line shape for pions with less than 80 MeV kinetic energy normalized to the corresponding data set. No statistically significant evidence for kaons is seen above the Landau tail on the pion line.

show the GEANT calculated line shape for pions with less than 80 MeV kinetic energy normalized to the corresponding data set. Within statistics, the observed pion line shape is consistent with this calculation.

Since the stopping detector is known for each particle event by event, a particle identification hypothesis can be checked against the energy observed in each detector element. Thus, for example, a particle identified as a pion with 120 MeV kinetic energy which appears to stop in the first 170 mm scintillator will be rejected since a pion of this energy must stop in the second 170 mm scintillator block. Range straggling effects are included in the simulations and therefore contribute to the overall detection efficiency.

The absolute energy calibration of the detector is based on well tracked, penetrating cosmic ray muons. Birks' Law [12], with parameters appropriate to the scintillator material, was used to relate detected scintillation light to deposited energy. This produces a slightly mass dependent energy calibration which we then check for consistency with the measured, and known energies at which each particle species makes the transition from one scintillator to the next along its entire range. The resulting energy calibration has a systematic uncertainty which is less than 6% for pions and less than 5% for protons and deuterons at all energies included in the final analysis.

The sides, top and bottom of the detector telescope were enclosed by 2.5 cm thick scintillator paddles. These detectors, which provided a nearly hermetic enclosure except for phototube penetrations, were operated with thresholds set to 300 keV and served to reject events in the off line analysis for which significant out-scattered energy was observed. For protons, deuterons and especially positive pions these events predominantly

involved in-flight hadronic interactions. In addition to in-flight interactions, a hadronic interaction occurs for each pionic atom formed by a stopped negative pion. Most of these events are also rejected by the 300 keV threshold. Although many of these rejected events would otherwise contribute correctly to Fig. 1, the recorded total energy deposition in the detector may be significantly shifted from the correct value. This is particularly true for π^- events where most of the pion rest mass is released at the stopping point in the detector. This excess energy deposition is further used to reject interacting particles and in particular events that form pionic atoms. A maximum and minimum energy bound is known for each particle species in each stopping detector.

From the discussion in the previous paragraph it is obvious that the telescope efficiency depends on the particle species and the particle energy. In particular, a significant intrinsic asymmetry exists between the detection efficiencies for π^+ and π^-. We have performed a full GEANT 3.21 simulation of the detector and target. Mono-energetic proton, deuteron and pion sources were chosen in GEANT to fill the telescope's fiducial acceptance and were tracked with all physics processes active. These calculations were used to correct measured energies for energy loss in the target and other inactive materials enroute to the detector and between the detector elements. The minimum kinetic energy for a given particle species used in the following analysis is based on these energy loss calculations. We somewhat arbitrarily impose the constraint that the maximum energy loss correction will in no case exceed 30% of the measured energy.

The particle identification algorithms generated for data analysis were applied to the GEANT output and used to produce energy dependent detection efficiencies for each particle species. For protons and deuterons the resulting detection efficiency is larger than 90% between 50 and 300 MeV kinetic energy and varies only weakly with energy. For π^+, the detection efficiency falls off at the lowest energies due to decay and multiple scattering losses and, at the highest energies included in the analysis, as a result of the onset of hadronic interactions in the detector material. The resulting detection efficiency within the fiducial acceptance for π^+ has a maximum of 67% and falls to 40% at 25 MeV and 31% at 110 MeV. The decay of stopped π^+ in the detector does not influence the detection efficiency to a significant degree but does slightly increase the overall detected π^+ energy at the lowest incident kinetic energies. Muon decays within the detector are excluded by the duration of the ADC gates (30 ns).

The detection efficiency for π^-, for reasons discussed above, is considerably lower. For our simulations we assume a ratio of 1:1 for the primary π^+/π^- ratio. Using identical GEANT calculations for π^- and π^+ detection we find the π^- efficiency to be 20% of the π^+ efficiency independent of energy. The magnitude of this ratio is determined by the details of the heavy particle (p,d,t,α) decay channels following the nuclear interaction that terminates each pionic atom. Therefore we take a conservative estimate of 25% as the uncertainty in the calculated π^- to π^+ detection efficiency ratio. This uncertainty, together with uncertainties in the detector's geometric acceptance, normalization, etc. is included in the overall systematic error of the measured yields. We compute a charged pion yield from our measured pion yields using the efficiency factors, as determined by the full GEANT calculations, to remove both the energy and charge

Table 1
The parameters of the three centrality cuts U1, U2 and U3 used in the present work. The range of the forward energy accepted, the resultant median impact parameter according to RQMD and the associated fraction (from experiment) of the geometric cross section selected by the cut are given

Cut	E_{ZD} range (GeV)	Median b (fm)	σ/σ_{geo}	Comment
U1	0–10	2.5	0.097	"central"
U2	10–60	4.5	0.301	"semi-central"
U3	$\geqslant$250	9.5	0.602	"peripheral"

dependence of the pion detection efficiencies. The uncertainty in the π^- to π^+ detection efficiency ratio is a small component in the total estimated systematic uncertainty of the charged pion absolute yield. It adds 5% to the absolute systematic error of 25% which is common to all detected particle species.

In addition to the scintillator array, the telescope incorporated a pair of Si surface barrier detectors mounted between the target and the first scintillator. A coincidence between these detectors served to define the fiducial acceptance of the telescope as a whole. The acceptance consisted of a cone of 1.9° half angle centered at 144° with respect to the beam. This provides a solid angle of 3.46 msr, small enough to guarantee negligible probability for multiple hits in a single event. By defining the acceptance of the telescope with the Si detectors, it was possible to oversize the scintillation detector elements in the transverse direction such that multiple scattering losses, particularly of pions, were minimized.

The silicon detectors were also used to provide a trigger for the data acquisition system. A beam flux of up to 5×10^4 per spill (1 s spill every 4 s) was used with a Pb target whose thickness was 2% of a ^{28}Si interaction length. Beam defining scintillators and the detection of a minimal interaction in the target region defined a pre-trigger sensitive to virtually all of the ^{28}Si+Pb geometric cross section. The presence of a coincidence between the pair of Si detectors generated a "telescope" trigger for the data acquisition system and saved the full event. Although an array of other triggers were utilized during the experiment, the present analysis is based solely on this telescope trigger.

For the measurements reported here, a hadronic sampling calorimeter (UCAL) functions as a zero degree calorimeter for centrality determination. The UCAL [13], which is located down stream of the E814 spectrometer magnet and 36 m from the target was studied in a GEANT calculation using RQMD events to model the relationship between detected forward energy, E_{ZD} and impact parameter. Measurements of the centrality dependence of the forward energy were reported elsewhere [14]. E_{ZD} is determined by integrating the energy in an angular range of $\pm 1°$ around the beam. A particular range of E_{ZD} is related to a range of impact parameter by tracking minimum bias RQMD events through the acceptance of the forward spectrometer and recording the relationship between the impact parameter, b, and E_{ZD}. We will discuss three centrality cuts based on the detected forward energy, E_{ZD}. Table 1 lists the properties of the three centrality

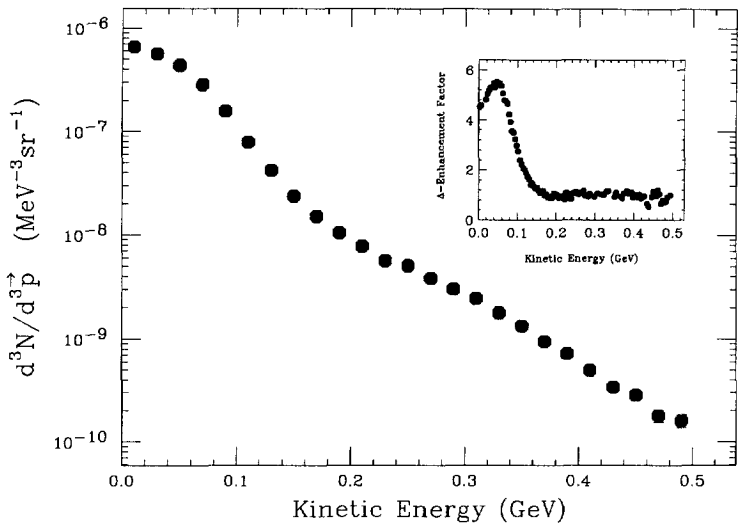

Fig. 2. The RQMD pion spectrum for central events in the telescope acceptance. The number of RQMD events corresponds to the number of recorded central events. The inset shows the RQMD spectrum divided by the thermal fit to $p_t > 300$ MeV/c, suggesting an enhancement of up to a factor of 6 at low momenta due to Δ decay

cuts U1, U2 and U3 used in the following analysis. These three centrality conditions may be characterized roughly as selecting central, semi-central and peripheral collisions, respectively.

3. Results and analysis

Previous measurements [15] in the backward rapidity range have been limited to protons and deuterons. Consequently, we will focus most of our discussion on the pion results. We will compare the experimental results with predictions from the event generator RQMD. Note that predictions from RQMD match well with experimental results on pion production at rapidities near and forward of mid-rapidity [10]. Charged pions with kinetic energies, T, in the range $22 < T < 150$ MeV are well identified and used in the present study. The associated pion rapidity interval thus studied is $-0.9 < y < -0.4$ and the transverse mass range is $7 < m_t - m_\pi < 67$ MeV/c^2. Fig. 2 shows the RQMD prediction for pions in our acceptance for very central ($b = 0$) collisions.

The data taken with the telescope detector determine the pion and nucleon cross sections at fixed laboratory angle θ, i.e. at fixed pseudo-rapidity η. To put the data into perspective we note that a thermally equilibrated source, centered at midrapidity and emitting isotropically at temperature T_B, i.e. $d^3N/d^3\boldsymbol{p} \propto \exp(-T/T_B)$, yields for pions at fixed laboratory angle θ a kinetic energy spectrum which is very close to a

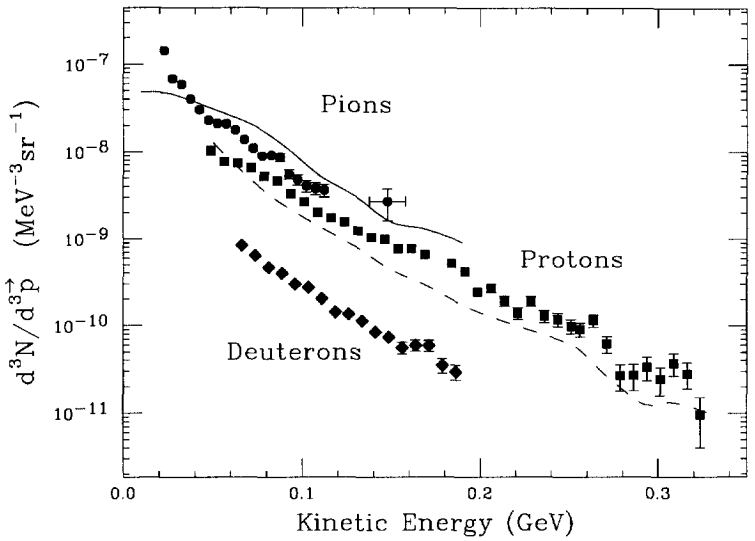

Fig. 3. Minimum bias yields of pions, protons and deuterons along with the corresponding RQMD calculations for pions (solid line) and protons (dashed line).

single exponential with an effective temperature parameter $T_{\text{eff}} = T_{\text{B}}/(\gamma(1 - \beta\cos\theta))$. Here, T_{B} is the source temperature, βc is the velocity of the midrapidity source in the laboratory system and $\gamma = 1/\sqrt{(1-\beta^2)}$. For a source at $y = 1.4$ this implies $\gamma = 2.15$ and $\beta = 0.89$ and $T_{\text{eff}} = T_{\text{B}}/3.7$ at $\theta = 144°$. Flow effects will of course modify the shape and slope of the spectra. We therefore do not only present a comparison to predictions for a thermally equilibrated isotropic source but mainly compare the data to an event generator (in this case RQMD) where the expansion dynamics is incorporated.

We note, in connection with Fig. 2, that our data are limited to pion kinetic energies of less than 150 MeV, and thus are sensitive almost exclusively to the Δ decay pion source which, according to RQMD, completely dominates over most of this energy range at this rapidity. Correspondingly, our measured energy range is insufficient to observe the strong spectral slope change predicted to occur near $T = 150$ MeV. On the other hand, as the inset to Fig. 2 shows, the predicted enhancement factor of the pion yield in our acceptance above the purely thermal yield is approximately a factor of 6 at $T = 60$ MeV. Thus a measurement of the pion cross section in this energy region is itself a stringent test of the importance of Δ decay for the pion yield. Furthermore, these measurements, in conjunction with previous measurements of the low p_t enhancement in pion spectra at forward rapidities, constitute at least a partial test of the rapidity dependence of pion spectra predicted if the dominant source of the pions is baryon resonance decay.

For the following comparison between event generator and recorded data, we generated as many minimum bias RQMD events as recorded events. The cuts were then applied to the simulated events in the same fashion than to the data.

Fig. 3 shows the minimum bias yield of charged pions obtained from the measured

Table 2
The inverse slope constants (T_{eff}) of pions, protons, and deuterons for different centralities. For minimum bias deuterons, protons, and pions the data are at mean rapidities of −0.24, −0.39, and −0.72, respectively. A single exponential in kinetic energy, T, is assumed with the fitting regions of $80 < T < 300$ MeV for protons, $65 < T < 190$ MeV for deuterons, and $50 < T < 120$ MeV for pions. The errors shown are statistical except for the deuteron slope parameter which includes a contribution from proton background subtraction. The χ^2 variation between the fits is less than 5%

Centrality Cut	T_{eff} (MeV)		
	Protons	Pions	Deuterons
Minimum Bias	45.1 (0.7)	31.6 (1.0)	36.4 (1.8)
U1	44.1 (1.0)	32.7 (1.6)	
U2	50.1 (3.0)	33.4 (1.8)	
U3	41.6 (3.0)	20.7 (0.8)	

pion yield as described above, and protons and deuterons in our acceptance. Here we plot the acceptance corrected momentum density $d^3N/d^3\boldsymbol{p}$ versus kinetic energy. The error bars as shown are statistical and are in addition to the 25% systematic uncertainty for protons and deuterons and 30% systematic uncertainty for charged pions.

All three curves are approximately exponential in kinetic energy with the exception of the lowest energy pions. These lowest energy pions are discussed further below. A fit to the proton spectrum in the range of 80 and 300 MeV yields an inverse slope parameter of $T_{eff} = 45.1 \pm 0.7$ MeV at a mean proton rapidity of −0.39 while the corresponding fit to the deuteron spectrum yields $T_{eff} = 36.4 \pm 1.8$ MeV at a mean rapidity of -0.24. The corresponding slope parameter for the minimum bias charged pion spectrum, fitted to the region above 50 MeV is $T_{eff} = 31.6 \pm 1.0$ MeV at a mean rapidity of −0.72. Assuming emission from an isotropic source this effective slope parameter yields a source temperature $T_B \approx 120$ MeV. We note, however, that for a single isotropic source we would expect that T_{eff} for protons is lower than that for pions at the laboratory angle of $\theta = 144°$, showing that isotropic emission cannot account for the present data. Longitudinal expansion [17] may be the origin of this difference.

In Table 2 we show a complete summary of slope parameters extracted from the present data including the centrality dependence for the case of protons and pions. Within errors, there is little or no significant centrality dependence of the proton inverse slope parameters. The pion spectrum, on the other hand, shows a significant steepening in peripheral collisions. The proton inverse slope parameter for central collisions is in good accord with the systematics established for Boltzmann temperatures as a function of scaled rapidity [16] for hadrons at both CERN and AGS. The corresponding pion inverse slope parameter is lower than that for protons, as can be seen in Fig. 2 for an energy range where the Δ decay contribution is large.

The dashed and solid curves in Fig. 3 are the corresponding minimum bias RQMD calculations for protons and charged pions, respectively. The calculations underestimate the proton yield and overestimate the pion yield (for $T > 40$ MeV) in each case by an amount slightly beyond our estimated systematic uncertainty. Further, the systematic

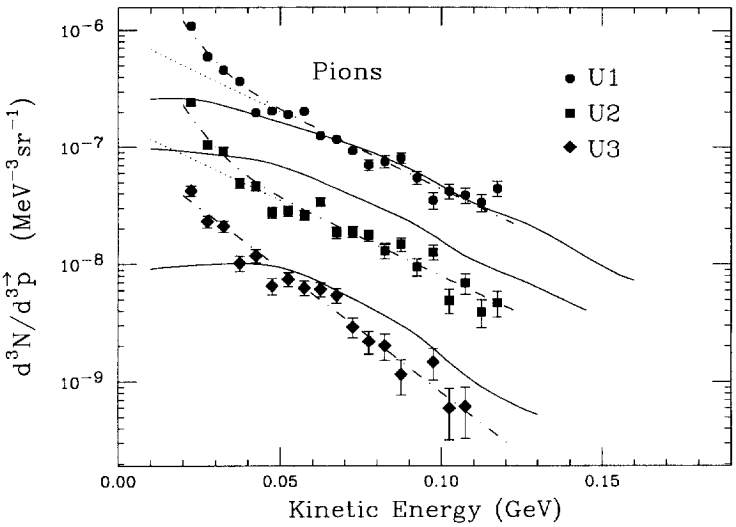

Fig. 4. The centrality dependence of the pion spectra for the centrality cuts U1,U2 and U3 discussed in the text and in Table 1. The solid lines are the corresponding RQMD calculations. The dotted line shown for the central (U1) and semi-central (U2) data shows a single exponential fit with inverse slope parameters T_{High} given in Table 3. The dash-dotted line shows the double exponential fit with T_{Low} and T_{High} as given in Table 3. For details see text.

errors in pion and proton yields are correlated and thus a real discrepancy exists between RQMD and our observed relative pion to proton yield. We will defer further discussion of both the proton and deuteron yields and their centrality dependence to a forthcoming article which will treat both the ^{28}Si+Pb and ^{197}Au+^{197}Au systems. Further discussion here will focus exclusively on the present pion results.

Fig. 4 shows the centrality dependence of the pion yields along with the corresponding RQMD predictions shown as solid lines. The centrality cuts are U1, U2 and U3 on the measured forward energy as described in Table 1. The slopes of the measured spectra are in reasonable agreement with RQMD at all centralities for $T > 50$ MeV including, as discussed further below, the correct evolution of the inverse slope parameters with centrality.

For $T > 60$ MeV the agreement between the shape of the pion spectrum and RQMD is acceptable, and the predicted enhancement due to resonance decays is indeed born out by the data. For example, the expected yield of pions is enhanced by a factor of 6 at 60 MeV due to Δ decay. Furthermore, Fig. 4 shows that the yields for centrally produced pions are described by RQMD within statistical uncertainties for kinetic energies of more than 50 MeV. We thus take the level of agreement seen in Figs. 3 and 4 as supportive of the rapidity dependence, which was predicted [6] as one of the identifying features of baryon resonances as the source of the pion low p_t enhancement.

Baryon resonances contribute at a much weaker level to K^+ production at AGS energies [6]. One of the consequences is that the rapidity distribution for kaons is

Table 3
Parameters determined from the double exponential fits to pion spectra for different centralities. $(dN/d\eta)_{\mathrm{Low}}$ and $(dN/d\eta)_{\mathrm{High}}$ are deduced from these fits by integrating in the kinetic energy range $22.5 > T > 117.5$ MeV. The effective temperatures obtained from spectra calculated with RQMD for the region $T > 60$ MeV are listed as T_{RQMD} and are to be compared with T_{High} deduced from the experimental data. The χ^2 variation between the fits is less than 5%

Centrality	T_{Low} (MeV)	T_{High} (MeV)	T_{RQMD} (MeV)	$\left(\frac{dN}{d\eta}\right)_{\mathrm{Low}}$	$\left(\frac{dN}{d\eta}\right)_{\mathrm{High}}$
U1	$8.0^{+2.0}_{-1.0}$	32.7 ± 1.6	34.5 ± 1.5	0.064	0.78
U2	$8.0^{+2.0}_{-1.0}$	33.4 ± 1.8	31.4 ± 1.4	0.013	0.14
U3	-	20.7 ± 0.8	23.4 ± 1.2	-	0.03

considerably narrower than that for pions. This should result in a K/π ratio in our rapidity range that is smaller than that observed near mid rapidity. The RQMD prediction for the K^+/π^+ ratio in our acceptance is 0.019 (compared to 0.2 at mid rapidity) which, given our statistics, is below our estimated sensitivity.

While the bulk of the pion cross section for kinetic energies $T > 50$ MeV is well accounted for in this rapidity range by RQMD where the dominant source is Δ decay (see Fig. 2), we also note a systematic feature of the pion yields which is distinctly at variance with the present calculations. For pion kinetic energies below about 50 MeV, the spectrum differs significantly from the RQMD prediction that d^3N/d^3p approaches zero slope at zero kinetic energy. This discrepancy with RQMD is independent of centrality and accounts for a significant fraction of the total pion yield. Considering just the centrally produced pions, for example, the integrated experimental yield of charged pions is $dN/d\eta = 0.95$ for $22.5 < T < 117.5$ MeV, in the η range covered by the detector, while the the corresponding integral from RQMD is $dN/d\eta = 0.65$. Of the total yield observed experimentally for charged pions, slightly more than 50% or $dN/d\eta = 0.56$ lies below $T = 50$ MeV.

In measurements with the Plastic Ball spectrometer, WA80 found evidence for an enhanced pionic yield at very low kinetic energy in backward hemisphere due to pion absorption in target spectator matter [18]. These data are well described by RQMD calculations, though. Our data suggest a low energy anomaly when compared to RQMD predictions, where (direct) thermal emission and resonance decays are simultaneously taken into account (Fig. 4, solid line). While a comparison of our results to a single exponential fit (corresponding to a thermal source at midrapidity) for the $T > 50$ MeV region (dotted line) is closer to the data in shape than the RQMD calculation, the fit clearly fails to account for the lowest energy pions for central and semi-central data. Allowing an additional source at lower temperature yields an adequate description of all the data with parameters as summarized in Table 3. Each fit is characterized by two inverse slope parameters T_{Low} and T_{High} and the corresponding integrated ($22.5 < T < 117.5$ MeV) source strengths $(dN/d\eta)_{\mathrm{Low}}$ and $(dN/d\eta)_{\mathrm{High}}$. The T_{Low} parameter is not fixed in these fits, but the errors listed in Table 3 give the full range over which

acceptable fits are achieved.

Both the central and semi-central charged pion spectra require a contribution characterized by an inverse slope parameter $T_{\mathrm{Low}} = 8$ MeV. This steep component amounts to approximately 10% of our integral yield in the range $22.5 < T < 117.5$ MeV. If we permit an extrapolation to $T = 0$ using the fit parameters from Table 3, then the strength of this ultra-soft component is not negligible and lies somewhere in the range of 10% to 50% of the total charged pion yield in our acceptance. This very low kinetic energy enhancement is absent or considerably weaker in the peripheral pion data. Fits to the peripheral data in Fig. 4 show an overall steeper slope but no evidence of an ultra-soft component.

The main body of the central and semi-central data presented here is characterized by the inverse slope parameter T_{High} which is in good agreement with the corresponding slope from RQMD as shown in Table 3. The ultra-soft pions are unexpected. There is, however, an experimental indication of a similar phenomenon in the E814 forward spectrometer data.

This additional observation of very low transverse momentum pions can be found in Ref. [10], which addresses low p_t pion production at forward rapidity. A close inspection of Fig. 1 of Ref. [10] reveals that, in addition to the low p_t enhancement predominantly due to Δ decay, a very steep slope is also visible at very low $p_t < 50$ MeV/c corresponding to $m_t - m_\pi < 10$ MeV/c^2. The inverse slope parameter of this ultra-soft component is comparable to the T_{low} deduced from the backward pion spectra in the corresponding range $T < 50$ MeV.

The observation of ultra-soft pions at forward rapidities in the forward spectrometer, and at fixed pseudo-rapidity in the backward hemisphere using a completely independent detector, suggest the possibility of a common origin.

Both measurements transcend present generation cascade calculations, implying that heavier baryon resonances or heavier mesons decaying into pions or kaons are unlikely sources of these ultra-soft particles. More exotic possibilities include, for example, mean field effects or the approach to chiral symmetry restoration which can produce very soft particle spectra as "light" mesons return to the mass shell as they emerge from the hot dense zone. These and other speculations are clearly not established at present but certainly provide ample motivation for further study of the very low p_t region in relativistic heavy ion collisions.

In conclusion, we have studied pion production at negative pseudo-rapidity in ^{28}Si+Pb collisions at the AGS using the E814 apparatus. The overall yield of pions is well described for kinetic energies $T > 50$ MeV ($p_t > 77$ MeV/c) by RQMD which predicts the dominance of Δ decay as the origin of these pions. This observation lends further support to the "resonance matter" interpretation of the pion low p_t enhancement seen in other rapidity ranges at the AGS. For kinetic energies $T < 50$ MeV, our spectral shape deviates significantly from predictions using RQMD. If the full pion energy range is described as a thermal spectrum then a very soft component is seen with effective temperature $T_{\mathrm{eff}} = 7$–10 MeV whose origin is unclear at present. This low temperature component is evident primarily for more central collisions. This feature which is apparent

at very low kinetic energy in the present data as well as in the transverse momentum spectrum for pions in the E814 forward spectrometer should be investigated in other rapidity ranges, for other particle species and various colliding systems.

Acknowledgements

We thank the AGS and Tandem staff and, in particular, Dr. H. Brown and W. McGahern for their excellent support. We also thank R. Hutter for technical support. This work was supported by DoE, the NSF, the NSERC (Canada), and the CNPq (Brazil).

References

[1] H. Sorge, H. Stöcker and W. Greiner, Ann. Phys. 192 (1989) 266.
[2] Y. Pang, T.J. Schlagel and S.H. Kahana, Phys. Rev. Lett. 68 (1992) 2743.
[3] See for example P. Braun Munzinger et al., Proc. NATO Advanced Study Institute on Hot Dense Matter, Bodrum Turkey, Oct. 93 eds. W. Greiner, H. Stöcker and A. Gallmann, (Plenum, New York, 1994) p.419.
[4] S. Kahana, Proc. Conf. on Heavy Ion Physics at the AGS, HIPAGS 93, eds. G.S.F Stephans, S.G. Steadman and W.L. Kehoe, MITLNS-2158.
[5] H. Sorge, R.Mattiello, H. Stöcker, W. Greiner, Phys. Lett. B 271 (1991) 37.
[6] H. Sorge, Phys. Rev. C 49 (1994) 1253.
[7] R. Brockmann et al., Phys. Rev. Lett. 53 (1984) 2012.
[8] G.E. Brown, J. Stachel and G.M. Welke, Phys. Lett. B 253 (1991) 19.
[9] W.A. Love et al. (E810 Collaboration), Proc. QM90, Nucl. Phys. A 524 (1991) 601c.
[10] J. Barrette et al. (E814 Collaboration), Phys. Lett. B 351 (1995) 93.
[11] J. Barrette et al. (E814 Collaboration), Phys. Rev. C 45 (1992) 819; Phys. Rev. C 50 (1994) 3047.
[12] J.B. Birks, The Theory and Practice of Scintillation Counting (MacMillan, New York, 1964).
[13] M. Fatyga, D. Makowiecki and W.J. Llope, Nucl. Instr. and Meth. A 284 (1989) 323.
[14] J. Barrette et al. (E814 Collaboration), Phys. Rev. C 46 (1992) 312.
[15] T. Sangster, J.B. Costales and M.N. Namboodiri (E859 Collaboration), Proc. Conf. on Heavy Ion Physics at the AGS, HIPAGS 93, eds. G.S.F Stephans, S.G. Steadman and W.L. Kehoe, MITLNS-2158.
[16] J. Stachel et al. (E814 Collaboration), Proc. QM 93, Nucl. Phys. A 566 (1994) 183c.
[17] P. Braun-Munzinger, J. Stachel, J.P. Wessels and N. Xu, Phys. Lett. B 344 (1995) 43.
[18] H.R. Schmidt et al. (WA80 Collaboration), Proc. QM91, Nucl. Phys. A 544 (1992) 449c.